

Continuous symmetry of C₆₀ fullerene and its derivatives

E.F.Sheka¹, B.S.Razbirin², E.A.Nikitina^{3,4}, D.K.Nelson²

¹ Peoples' Friendship University of the Russian Federation, 117198 Moscow, Russia

² A.F. Ioffe Physical-Technical Institute, RAS, 194021 St.Petersburg, Russia

³ Photochemistry Center RAS, 119421 Moscow, Russia

⁴ Institute of Applied Mechanics RAS, 119991 Moscow, Russia

Abstract. Conventionally, the I_h symmetry of fullerene C₆₀ is accepted which is supported by numerous calculations. However, this conclusion results from the consideration of the molecule electron system, of its odd electrons in particular, in a close-shell approximation without taking the electron spin into account. Passing to the open-shell approximation has lead to both the energy and the symmetry lowering up to C_i . Seemingly contradicting to a high-symmetry pattern of experimental recording, particularly concerning the molecule electronic spectra, the finding is considered in the current paper from the continuous symmetry viewpoint. Exploiting both continuous symmetry measure and continuous symmetry content, was shown that formal C_i symmetry of the molecule is by 99.99% I_h . A similar continuous symmetry analysis of the fullerene monoderivatives gives a reasonable explanation of a large variety of their optical spectra patterns within the framework of the same C_i formal symmetry exhibiting a strong stability of the C₆₀ skeleton.

Key words: continuous symmetry; electronic spectra; semi-empirical quantum-chemical calculations; fullerene C₆₀ derivatives

1. Introduction

Fullerene C₆₀ is related to those rare molecules, whose structure had been predicted before the molecule was discovered experimentally. The first suggestion was made by Jones in 1966 who assumed that intercalation of pentagon defects into a plain graphite layer (graphene according to the nowadays nomination) consisting of perfect hexagons would result in the transformation of this layer into a closed hollow shell that presents a giant carbon molecule [1]. In 1970 Osawa published a short communication [2] showing a possibility of existing C₆₀ molecule in the form of truncated icosahedron, consisting of 60 atoms. Next year Osawa and Yoshida discussed possible aromatic properties of the molecule [3]. Two years later Bochvar and Galpern [4] as well as Stankevich and coworkers [5] performed calculations of the molecule electronic structure. This calculation repeated in a few years by Davidson [6], showed that the closed-hollow-cell C₆₀ molecule is characterized by a large distance between the energies of the highest occupied (HOMO) and lowest unoccupied (LUMO) molecular orbitals, which points to a chemical stability.

The first discovering of the molecule is usually connected with the names of Kroto, Curl, and Smalley (KCS) [7] although a year earlier its presence among carbon clusters was heralded [8]. Not knowing the above cited results, KCS suggested a truncated icosahedron shape of the molecule, consisting of 32 faces, 60 apices (carbon atoms), and 90 ribs. Supposing a full equivalence of atom positions, the symmetry of the polyhedron as a geometrical replica for equilibrium positions of the molecule atoms was attributed to the point-group symmetry I_h . This suggestion has laid the foundation of a doubtless view on the molecule shape symmetry that has been supported by now by the absolute majority of the fullerene community in spite of a number of contradictions to this paradigm when interpreting some of the molecule properties. All the inconsistencies with the high symmetry are usually considered in terms of “a slight lowering of the molecule symmetry from the ideal symmetry I_h under particular conditions”. In the current

paper we advocate a new consideration of the molecule property showing that there are serious reasons in the ground of these contradictions so that the symmetry problem of fullerene C₆₀ is not so simple.

2. C₆₀ shape and symmetry: Structural experiments

As accepted, the most reliable atomically mapped description of the molecule structure follows from the gas phase electron diffraction (EGD) [9]. Actually, the diffraction pattern is well fitted when suggesting that the molecule shape is a truncated icosahedron of the point-group symmetry I_h , which is formed by two types of C-C bonds, ones of a substantial double bond character and of $h=1.398(10)$ Å in length while the other are of $p=1.455(6)$ Å long and have a prevalent single bond character. Sixty carbon atoms are arranged in 20 six-membered and 12 five-membered rings. The C-C bonds separating two hexagons are double bonds (h) while the pentagon C-C bonds (p) are single. Under the same suggestion a good fitting to experimental data related to neutron diffraction (ND) from C₆₀ powder [10] and X-ray data (XRD) for the C₆₀ crystal [11] was obtained. The available data concerning C-C bond length are collected in Table 1. Analyzing the data, one can conclude that EGD provides the most accurate bond length determination whilst its accuracy is of 10^{-2} Å only [9, 14]. At the same time, ND and XRD methods do not allow determining the value better than 10^{-1} Å.

3. C₆₀ shape and symmetry: Quantum-chemical calculations

The modern Born-Oppenheimer-approached quantum chemistry can provide the accuracy in the bond length determination not worth than of 10^{-5} Å. That is why quantum-chemical calculations can be regarded as highly accurate structure determination technique under conditions when a complete set of calculated results fits experimental findings of the object under consideration. Starting from [15, 16], the molecule has been repeatedly and thoroughly studied computationally (see [17-20] and references therein). In some sense, C₆₀ turned out to be a proving ground for testing different computational techniques, from a simplest to the most sophisticated. However, all calculations were based on the aromaticity concept which revealed itself in a close-shell or restricted approximation. All calculations have shown I_h -symmetry of truncated icosahedron structure to be corresponded to the lowest potential energy minimum in the singlet state. However, as was thoroughly discussed in [13, 21], the length of the molecule long C-C bonds exceeds the region that provides a complete covalent bonding of odd electrons, so that a remarkable difference ΔE^{RU} in the energies of restricted and unrestricted solutions should be expected highlighting non-stability of the restricted solutions and positioning a stable pure spin and physically real ground state of the molecule at lower energy. This is so indeed and Table 2 presents data based on single-determinant Hartree-Fock (HF) calculations. To show that the same happens for other fullerenic structure, data for C₇₀ and Si₆₀ molecules are added to the table.

As seen from the table, spin-contaminated energies of the unrestricted broken symmetry HF (UBS HF) solutions and pure spin energies of all three molecules are much lower than those of the restricted solutions. The ΔE^{RU} values constitute 1.53, 3.85, and 22.9% the RHF heats of formations for C₆₀, C₇₀, and Si₆₀, respectively. The finding points that the restricted solution is unstable in this case while unrestricted solution with lower energy is evidently closer to the physical reality. However, the energy lowering exhibits not only the instability of the restricted solution but is followed by the symmetry lowering as well. A tight connection between the energy lowering and the molecule symmetry has been thoroughly discussed in [25-32]. Since that it is commonly believed that the energy lowering is generally accompanied by a descent of symmetry (which adds geometry and/or symmetry instability to the spin instability). That is why

lowering I_h symmetry of RHF solution of C_{60} to C_i symmetry of the UBS HF one does not look quite unexpected.

Since the real state of the molecule is spin pure and since its energy is lower than that of spin-contaminated UBS HF one, the real symmetry of the molecule cannot be higher than the symmetry of the UBS HF state. That is why the UBS HF symmetry of the species is suggested for pure spin states in Table 2. A final decision on the real symmetry of the molecule might be put on shoulders of experiments. However, this way turned out to be rather complex and ambiguous. The situation is not particularly typical for fullerene species and is well known for other cases such as a discussion about D_{6h} and/or D_{3h} symmetry of the benzene molecule [33].

In the case of C_{60} , the statement that the point group symmetry of the molecule is C_i seems to drastically contradict to the common opinion. Actually, a beautiful geometrical truncated-icosahedron shape seems do not allow even thinking about the molecule symmetry lower than I_h . And this intuitive expectation is considered to be proved by direct structural experiments and quantum chemical calculations. But any experimental proof has never been an absolute one providing a rigid “yes/no” answer concerning physical object symmetry due to unavoidable uncertainties inherited in experimental data. The latter is related even to such sophisticated technique as quantum chemical calculations where, as seen from Table 2, application of restricted approach instead of unrestricted one results in erroneous lifting of the molecule symmetry.

At the same time, the analysis of the molecule structure corresponding to either RHF or UBS HF solutions makes it possible to manifest what means the C_{60} symmetry lowering from I_h to C_i . Both approaches support the molecule truncated icosahedron shape formed by two groups of C-C bonds of different character. Thus, short bonds are close to the double bonds, which might be characterized by the Wiberg bond index [34]. In both cases the average Wiberg index for the bonds is 1.494 similar to that in benzene. As for long bonds, the average Wiberg index of 1.10 clearly evidences the single bond character. Therefore, the symmetry lowering is not connected with changing either the molecule shape or C-C bond character and is concerned with more delicate quantitative characteristics. Such is indeed the case, and the changing concerns the scattering of C-C bonds lengths. Figure 1 presents the dispersion of C-C bond distribution for two molecular structures that correspond to RHF and UBS HF solutions. As seen from the figure, if the average values of the bond lengths practically coincide for long bonds and slightly differ for short ones, the corresponding dispersions differ many times (four-time and 16-time for long and short bonds, respectively). This large difference in the bond length dispersion strongly actualizes the question concerning uncertainty of structural experiments performed since the two symmetry-different structures can be distinguished if only the accuracy of the bond length determination is better than 10^{-2}\AA . As for the most accurate EGD experiments [9, 14], their accuracy is close to the limit. However, a great number of adjustable parameters used under interpreting the data attenuate a confidence in the objective persuasiveness of the conclusion in favor of I_h symmetry. A precise determination of the molecular geometry by neutron scattering from C_{60} powder [10] gives values $h=1.391\pm0.063\text{\AA}$ and $p=1.452\pm0.066\text{\AA}$ that are even less accurate from the experimental viewpoint. The same can be addressed to the XRD data for the C_{60} crystal [11]. Therefore, structural experiments are really not discriminative for the case and cannot resolve structures with either I_h or C_i symmetry.

Electronic optical spectra are another source of information related to the point-group symmetry. An exhausted and detailed analysis of highly structure-sensitive low-energy $S_0\rightarrow S_1$ electronic optical spectra of C_{60} forced the authors of review [35] to conclude that in spite of a high-symmetry pattern of the spectra as a whole, some peculiarities, such as a weak pure electronic 0_0^0 transition in both absorption and fluorescence spectra, the vibronic series in the latter spectrum based on g -symmetry vibrations, absolutely allowed pattern of the phosphorescence spectrum, the “silent” modes in Raman and IR spectra [36], and others are inconsistent with the high symmetry of the molecule and cast some suspicion on the point.

The conclusions made on the basis of spectral studies as well as discriminative inability

of structural experiments could seemingly be ponderable arguments in favor of the point-group symmetry C_i although a high-symmetry pattern of the molecule spectra require an additional explanation. This fact as well as other physical reality shows that the symmetry problem of fullerene C_{60} cannot be solved in terms of exact symmetry. A further evidence of the problem actuality was obtained when studying optical spectra of fullerene C_{60} monoderivatives. Figure 2 presents three pairs of specular absorption/luminescence spectra belonging to molecules C_{60} and two its monoderivatives dissolved in crystalline toluene. The spectra manifest the Shpol'skii effect, which concerns fine structure of vibronic spectra of soluted molecules in crystalline matrices under particular conditions [37]. The monoderivatives differ by added atomic groups that are shown in Fig.3. A high-symmetry pattern of the pristine fullerene spectra in Fig.2c is obvious: a very low intensity of the pure electronic 0_0^0 bands in both spectra and the dominance of vibronic series based on non-totally u -symmetric vibrations that is Herzberg-Teller (HT) pattern. This pattern is typical for high symmetry molecules with forbidden or slightly allowed electron transitions (see spectra of benzene and naphthalene for example [41]). It is usually accepted as a convincing experimental evidence of high symmetry of the molecular object under study. If one might expect the pattern for C_{60} basing on its overestimated symmetry, the symmetry of both derivatives is evidently C_1 , which does not imply any forbidness of electronic transitions, so that their spectra should drastically differ from that of pristine fullerene. As turned out, the reality does not follow the expectation completely. Actually, as seen in the figure, the spectra of species **I** are absolutely different from those of pristine fullerene, while the spectra of species **II** are quite similar to the latter. The difference between spectra of C_{60} and **I** concerns not the detailed vibrational structure of the spectra, which is expected, but the shape of the total spectra. Thus, a high-symmetry HT pattern of the C_{60} is substituted by the Frank-Condon (FC) pattern that is characterized by intense 0_0^0 bands and vibronic series based on g -symmetric vibrations only [42]. Oppositely to the case, spectra of species **II** preserve the HT pattern and a close similarity to the spectra of C_{60} . The only difference concerns the vibronic structure itself due to an obvious difference in vibrational modes of both molecules. Therefore, a low symmetry molecule **II** is characterized by a high-symmetry pattern of its electronic spectra.

The finding clearly shows up that the problem concerning the symmetry of the C_{60} skeleton is not simple. The notations C_i or C_1 themselves do not mean much since the matter is evidently not about these exact “yes/no” symmetries but about how much they both differ from, say, the I_h -one. The situation is not unique in the molecular world but the exclusive position of the fullerene forces to draw a particular attention to the problem. A concept based on the continuous symmetry approach seems to be the most suitable tool for the problem elucidation.

4. Continuous symmetry concept

A highly heuristic view that symmetry can be and, in many instances, should be treated as a continuous “gray” property, and not as a “black or white” one which exists or does not exist, was introduced by Zabrodski, Peleg, and Avnir (ZPA) in 1992 [43, 44] and thoroughly elaborated further by Prof. Avnir team as quantitative tools for the continuous symmetry measure (CSM) [43, 45], continuous chirality measure (CCM) [46], and continuous shape measure (CShM) [47, 48]. However, the topic has not been widely accepted so far and still is of interest of a rather narrow group of scientific community, mainly chemical theoreticians [43-53], while the majority of practicing chemists and physicists still prefer “black and white” approach. Speaking about continuous symmetry, the ZPA approach does not restrict oneself by the object symmetry and shape but concerns mass or electronic distributions as well. It means that *continuous symmetry* should be determined not only for the object shape but also for other massifs of data that provide the description of molecular properties on matrix-element level [52, 54]. However, usually, the shape symmetry is considered as basic one that strictly governs all other object properties.

As thoroughly analyzed in [55], the exact symmetry conceptual inflexibility which demands “yes or no” answer bends a rich reality of stereochemistry to the dictates of a strict codex, behind which are hidden (1) the paradigm that exact symmetry is superior and therefore must set the rules and (2) the practical aspect that fully symmetric situations are easier to formulate theoretically. The strict codex of perfect symmetry is particularly devastating in the case of small deviations from symmetry that force a jump in the symmetry description, the magnitude of which is totally out of proportion from that deviation. At the same time the continuous symmetry concept makes it possible to replace a conventional question: “What is the object symmetry under such or other conditions?” by another one: “How much the symmetry of the object deviate from an ideal and/or reference one under such or other conditions?” If the answer to the latter can be quantified, one can expect to be able to substitute usually met statements like: “The NH group perturbs the electron system of C₆₀ molecule to a small extent” (with respect to the intensity of the lowest electronic transition in Fig. 2) by some quantitative structure-property correlations. The continuous symmetry approach can satisfy these expectations to the most extent.

Mathematically, the approach is based on the distance-function formulation that makes it possible to determine a set of useful quantitative characteristics [43, 46, 55-58]. The first is the *continuous symmetry measure* CSM that is a distance function commonly employed in the symmetry analysis. If M is a structure composed of n vertices (atoms) in an original configuration, Q_i , and G is any symmetry point group, the amount of G -symmetric shape in M is defined as [55]

$$Sy(M, G) = \frac{1}{nD^2} \sum_{i=1}^n \|Q_i - P_i\|^2. \quad (1)$$

Here P_i are the searched corresponding points of the nearest G -perfectly symmetric configuration, and D is a size normalization factor (the *rms* of all distances from the center of mass to the vertices), making Sy size-invariant. The distance $Q_i - P_i$ is squared to avoid sign limitation, as is a common practice in distance-function formulations. The bounds of Sy are 0 (Q_i coincides with P_i ; M is perfectly symmetric) and 1 (the nearest symmetric structure coalesces onto a center point, the distance to which is 1). To make the values more sensitive to the geometry deviation, the latter are usually scaled by 100. Several algorithms were developed for the identification of P_i and implemented in working programs SYMMETRY and SHAPE [59]. $Sy(M, G)$ is a quantitative description of CSM within 0-100 scale.

The *continuous symmetry numbers* (CSNs) is the next distance function which measures the deviation from rotational symmetry. Originally they were introduced as

$$\sigma = \sum_k r_k. \quad (2)$$

to correct evaluation of rotational entropy [56]. Here k numbers proper C_n rotations and

$$r_k = 1 - Sy_k \quad (3)$$

where Sy_k evaluates the degree of a specific rotation operation k from perfectness and is expressed as

$$Sy_k(M, k) = \frac{1}{nD^2} \sum_{i=j}^n \|Q_i - P_{ik}\|^2. \quad (4)$$

The distance function Sy_k should be determined for each of k symmetry elements of the point group G within the interval from 0 to 1. Obviously, the last three equations can be expanded over improper rotations S_n , inversion (S_2), mirror symmetry C_s , and chirality C_h thus allowing determination of *continuous symmetry level* (CSL) σ_{cont} (the term was suggested by D.Avnir and C.Dryzhun and accepted by the authors with gratitude). When the set of symmetry elements of the point group G is formed of the above elements, CSL σ_{cont} describes an absolute contribution of the G -symmetry in the studied structure while $\eta_{cont} = \sigma_{cont} / \sigma_{classic}$, where $\sigma_{classic}$ equal to k is a perfect measure of the G -symmetry, presents a relative contribution.

A complex of programs created in the Hebrew University of Jerusalem [59] offers a large possibility to determine a consistence of shapes of two structures by SHAPE program, to find a selected point group symmetry contribution into a studied structure by SYMMETRY program and to evaluate chirality of the structure by CHIRALITY program. Let us look at pristine fullerene C_{60} and its derivatives from the viewpoint of continuous symmetry.

5. Fullerene C_{60} and its monoderivatives

The first application of the continuous symmetry concept to fullerene C_{60} concerned the symmetry of its anions from C_{60}^{-1} to C_{60}^{-6} [55]. Classically, the structural change induced in C_{60} upon charging to C_{60}^{-1} is associated with an abrupt drop in symmetry from I_h to D_{3h} , which leads to a grossly overestimated rotational entropy change and to CSN σ_{cont} , limited by proper rotations, equal to 60 and 6, respectively. Similar abrupt changes without any reasonable order, as well as grossly overestimated values of rotational entropy changes, are also obtained for the rest of other anions toward C_{60}^{-6} . At the same time, changes in CSNs, calculated for rotations involved in the rotational subgroup of the point group I_h , for all anions (σ_{cont} lies in the interval from 58.73 to 58.72) constitute only 2.2% instead of 90% expected classically. This means that the anion C_{60} skeleton preserves the I_h -ness to a great extent.

In the current paper we proceed with the consideration of the C_{60} fullerene symmetry and address the symmetry measure to answer two questions: 1) how much C_i - structure of the molecule, which follows from the UBS HF solution, deviates from the I_h -structure of the RHF solution and 2) how much I_h symmetry contributes to structure of various C_{60} monoderivatives as a whole and to their C_{60} skeletons, in particular. Answering the first question, we use two continuous symmetry measures provided by programs SHAPE and SYMMETRY. In the first case, the corresponding symmetry measure $Sy(M, G)$ was obtained in due course of the comparison of the molecule C_{60_RHF} (I_h) and C_{60_UBS} HF (C_i) shapes. The CSM analysis was provided by the same fixed numeration of the molecule atoms in both structures. In its turn, Sy_k values, provided by the SYMMETRY program, allowed evaluating the response of C_i -structure on each symmetry element of I_h point group. The consideration of the fullerene derivatives was carried out in terms Sy_k .

The application of the shape symmetry analysis to C_{60_RHF} and C_{60_UBS} HF structures gives the $Sy(M, G)$ values equal to 0 and 0.011951, when either identical or different structures are compared. If $Sy(M, G) = 0$ points to a trivial identity of the structure compared with oneself,

$Sy(M, G) = 0.011951$ (0-100 scale) evidences a practically negligible deviation of the C_i -structure from the I_h -one.

Eight symmetry elements of I_h point group are given in the top of Table 3. All of them, beside symmetry planes σ , can be directly tackled within the SYMMETRY program to obtain corresponding Sy_k values. As for the planes, those are perpendicular to C_2 axes, so that we can consider them via chirality's element C_h . The table contains symmetry measures Sy_k determined according Eq. (4). The numbers are given in 0-1 scale.

The values related to C_{60_RHF} (I_h) are equal zero, as should be expected. Sy_k values for C_{60_UBS} HF (C_i) differ from zero starting from the fourth and/or fifth digits after the point. However, the deviation is actually small that is why a summary σ_{cont} constitutes 119.99 instead of $\sigma_{classic} = 120$ and $\eta_{cont} = 99.99\%$. Therefore, the C_i -structure is practically of I_h symmetry. This finding correlates perfectly with the data of the shape analysis. A similar conclusion seems to be expected for the real symmetry of the C_{60} molecule in the pure spin singlet state, which formally cannot be higher than the exact C_i symmetry of the UBS HF solution but in terms of continuous symmetry should be predominantly I_h . The high continuous symmetry of the molecule provides high-symmetry patterns of all the symmetry sensitive experimental recordings. At the same time, its deviation from the exact I_h symmetry may be used to explain all the inconsistencies of experimental recordings from the exact high-symmetry ones.

As for fullerene derivatives, the continuous symmetry measure analysis makes it possible to trace changes in both the derivative as a whole and its C_{60} skeleton when an atomic group is added to the pristine fullerene. Let us look at the relevant data for the structures shown in Fig.3 which are presented in Table 3 and Table 4. The data related to the molecules themselves are bolded. As seen from the table, all additions considerably disturb the molecule structures so that their deviations from the I_h -one are quite large. Actually, σ_{cont} in Table 4 changes from 113.128 to 86.129 resulting in η_{cont} laying in the interval from 94.3 to 71.8%. In its turn, the expansion of the changes over symmetry elements in term of Sy_k in Table 3 forms the ground for a new 'symmetry language' for the change description as well as for its comparative analysis with respect to varied structure and composition of the added groups. This makes it possible to substitute usually met a typical sentence such as "CH₃ unit causes a rather weak effect on the benzene ring structure" by another one: " C_s symmetry of toluene molecule preserves 77% symmetry with respect to C_6 operation, 80% of C_3 , 98% of C_2 , 92.3% of inversion, 100% of C_s , thus conserving ~92% of D_{6h} symmetry in total". Similarly, the data presented in Table 3 may be used to describe C_i symmetry of the discussed derivatives. It is clearly from the table, that a concrete content of this description is different for the molecules characterized by different addends, in spite of the fact that the latter are added to the same atoms of the pristine fullerene cage.

Oppositely to the whole molecules, their C_{60} skeletons having C_i exact symmetry in all cases preserve (99.99÷99.98) % of I_h symmetry, as follow from Tables 3 and 4. Therefore, the same molecule may produce both low-symmetry and high-symmetry experimental patterns depending on which atoms are involved in the empirical response. If those are skeleton atoms only, one obtains a high-symmetry patterned response. If addend atoms are mostly involved, a low-symmetry patterned response will be obtained. Let us consider this effect exemplified by optical electronic spectra of the studied derivatives.

6. Optical electronic spectra of fullerene C_{60} and its derivatives

The considered electronic spectra correspond to optical transitions between the ground and excited electronic states produced within the first HOMO-LUMO gap [35]. In the framework of

single-determinant HF approximation, the atomic function composition of HOMO and LUMO will govern the atomic-sensitive characteristic of the wave functions of excited states. Table 5 presents a percentage contribution of addend atoms in HOMOs and LUMOs of the studied derivatives. As follows from the table, the addend atoms do not contribute to LUMOs in all cases. As for HOMO contributions, the latter is zero for molecule **II**, constitutes 0.9÷1.4% for molecules **III**, **IV**, **I** and absolutely dominates at the level of 97.1% for species **V**. The data obtained allows for making certain conclusions concerning optical spectra of the molecules.

1. Spectra of molecule **II** are governed by the participation of C₆₀ skeleton atoms only so that the spectra pattern should be similar to that of the pristine fullerene.
2. Spectra of molecules **I**, **III**, and **IV** are initiated by both C₆₀ skeleton atoms and addends so that the whole molecule is responsible for the spectra intensity. Suggesting that the intensity would correlate with the deviation of the molecule structure from *I_h*-symmetry (taken as a measure of the *C_i*-ness in terms of *I_h* symmetry), the intensity should increase when going from molecule **IV** (16%) to **III** (17%) and then to **I** (25%). At the same time intensity of spectra, which correspond to the excitation of the lowest excited state, should be compared with that of pristine fullerene due to low contribution of the addend atoms into the relevant HOMOs.
3. Spectra of molecule **V** should have a spectral-allowed pattern and be of the highest intensity due to both a high measure of the *C_i*-ness (19.9%) and a high addend atom contribution to the HOMO.

These predictions are supported by direct calculations of the oscillator strength related to optical dipole transitions to the first low lying excited states. The data obtained in the framework of ZINDO/S method [60] implemented in the GAUSSIAN package [61] for molecular structures shown in Fig. 3 are given in Table 6. The table lists five lowest excited states that contribute to low-frequency optical absorption spectra of the species [35]. As seen from the table, both *I_h*- and *C_i*-structures of C₆₀ are characterized by zero oscillator strength of electronic transitions in this region. This might be interpreted that in spite of a formal allowance of the transitions for the *C_i* molecule, its wave functions are in fact enough highly symmetrical to provide zero dipole matrix elements related to the transitions. This appears to be consistent with the symmetry analysis discussed earlier.

The remaining five molecules are characterized by allowed transitions in the region, summary intensity of which forms a series **V** > **I** ≥ **IV** > **III** > **II**. It should be noted that when summary intensities of the transitions of molecules **V**, **I**, and **IV** are comparable, those of species **III** and **II** are two-three times less. The series is fully synchronous with that one presenting the deviation of the molecule symmetry from the *I_h* one as follows from Table 4. Actually, following the disclosed tendency **V** > **I** ≥ **IV** > **III**, one can see a synchronous directed changing in the spectra pattern of molecules **V**, **I**, **IV**, and **III** presented in Fig. 4. The spectra of first three molecules have a clearly exhibited FC vibronic pattern and their intensity somewhat decreases downward, accompanying with a simultaneous extension of the spectra vibronic structure of the luminescence spectra. Thus, in the case of molecule **V**, zero-vibration (pure electronic) 0₀⁰ band dominates in the spectrum while its vibrational repetitions are rather scarce. The same retains in the case of molecules **I** and **IV** with the domination of the 0₀⁰ band slightly decreased. Oppositely to the cases, spectra of molecule **III**, whose intensity differ twice from those of the above mentioned molecules, are of different shape; the 0₀⁰ band in both absorption and luminescence spectra constitutes an ordinary part of extended vibronic series that are a mixture of FC and HT series in the favor to the former so far starting with a rather weak but still clearly vivid 0₀⁰ band [31]. This dependence of spectra vibronic structure on the intensity of electronic transition is a typical feature in molecular spectroscopy of large molecules where weak electronic transitions are presented by extended series of vibronic bands oppositely to strong allowed transitions. This is connected with the fact that in the former case there is a comparable chance for a number of different vibrations to be exhibited, including both *g*- and *u*- symmetric vibrations. Oppositely, in

the latter case, the vibrational repetitions are provided by a limited number of g -symmetric vibrations only, series extension of which is determined by the shift of the equilibrium positions of atoms under the electronic excitation. For large molecules the latter is usually small, which results in short vibronic series. Spectra of molecule **V** in Fig.4a clearly demonstrate the latter tendency, particularly, for the luminescence partner. Lowering intensity for molecules **I** and **IV** produces a vivid extension of the vibronic structure of their spectra (Figs.4b and 4c) while a further lowering the intensity of the electronic transitions for molecule **III** causes a substantial enrichment of the vibronic structure transforming it into a mixture of FC and HT series, so that it becomes quite similar to a rich vibronic HT structure of electronic transitions of the pristine fullerene C_{60} spectrum.

Figure 5 presents spectra of molecules **III** and C_{60} in more details based on fine-structured Shpolskii's spectra at 2K. Unfortunately, due to very strong tendency to clusterization (see for example [62]), molecules **II** cannot be distributed in the toluene matrix as individual entities, which prevents from obtaining their fine-structured vibronic spectra similar to those of molecules **III** and C_{60} so that even at low temperature its spectra consists of rather broad bands (Fig. 5c). As clearly seen in Figure 5a and 5b, spectra of both molecules present a mixture of FC and HT series with the difference that when the FC series is the most intense in the former case, the HT series dominates in the latter. Lowering the absolute intensity when passing from molecule **III** to C_{60} inhibits the intensity of the FC series. The same happens when going from molecule **III** to **II** since the spectra of the latter are just overlapping of those of C_{60} .

Basing on the finding it might be said that summary strength of the electronic transitions at the level between 0.005 and 0.006 which is characteristic for **II** and **III** (Table 6) can be considered as a limit for a transition from a predominantly forbidden HT spectra pattern to predominantly allowed FC one. In the studied case this corresponds to 10-15% deviation from the highest I_h symmetry. Therefore, '(0.006-0.005)/(10-15)%' relationship seems to be a bordering condition when changing in structure-symmetry of a fullerene molecule will cause a qualitative reconstruction of its optical spectra that allows establishing a lifting and /or lowering of the molecule symmetry. Similar quantitative relationships can be established for other structure-sensitive experimental techniques such as NMR, IR and Raman spectroscopy, etc. Evidently, quantitative expressions for bordering cases might be different for different techniques.

7. Conclusion

Continuous symmetry approach may be suggested as a new 'symmetry language' that provides a quantitative description of a molecule structure in terms of higher symmetries and forms the grounds for establishing quantitative structure-property relationships. Optical spectra offer a good platform for the latter due to their high sensitivity to structure deviation. Applied to C_{60} fullerene and its monoderivatives, the approach has proved its great efficiency and has highlighted a big stability of the fullerene skeleton, the deviation of whose symmetry from I_h is rather small even with respect to non-symmetrical additions of various molecular units.

Acknowledgement

One of the authors (E.Sh.) is grateful to S.S.Trach for attracting her attention to a quantitative approach for molecule symmetry consideration. A particular gratitude to D.Avnir, C.Dryzhin, and M.Pinsky for numerous fruitful discussions, for presenting a possibility to be acquainted with programs SHAPE and SYMMETRY, for giving permission as well as invaluable practical lessons of the programs use. The work was partially financially supported by the RFBR (grant № 07-03-00755).

References

1. Jones, D.E.H. Ariadne. *New Scientist*. 32: 245 (1966).
2. Osawa E. Kagaku (Kyoto) 25, 854 (1970).
3. Yoshida, Z.; Osawa, E. *Aromaticity*. (In Japanese).174. Kyoto: Kagaku Dojin. 1971.
4. Bochvar, D.A.; Galpern, E.G. *Doklady Physics* 209, 610 (1973).
5. Stankevich, I.V.; Nikerov, M.V.; Bochvar, D.A. *Russ. Chem. Rev.* 53, 640 (1984).
6. Davidson R.A. *Theor. Chim. Acta*. 58, 193 (1981).
7. Kroto H.; Heath J.R.; O'Brien S.C.; Curl R.F.; Smalley R.E. *Nature* 318, 354 (1985).
8. Rohlffing E.A.; Cox D.M.; Kaldor A. *J.Chem. Phys.* 81, 3322 (1984).
9. Hedberg, K.; Hedberg, L.; Bethune, D.S.; Brown, C.A.; de Vries, M.; Dorn, H.C.; Johnson, R.D. *Science* 254, 410 (1991).
10. Leclercq, F.; Damay, P.; Foukani, M.; Chieux, P.; Bellisent-Funnel, M.C.; Rassat, A.; Fabre, C. *Phys. Rev.* 48B, 2748 (1993).
11. Slovokhotov, Yu.L.; Moskaleva, I.V.; Shil'nikov, V.I.; Valeev, E.F.; Novikov, Yu.N.; Yanovski, A.I. ; Struchkov, Yu.T. *Mol.Mat.* 8, 117 (1996).
12. Yanonni C.S., Bernier, P.P. ; Bethune, D.S. ; Meijer, G. ; Salem, J.K. *J.Am.Chem.Soc.* 113, 3190 (1991).
13. Sheka, E.F. *Int.Journ.Quant.Chem.* 107, 2361 (2007).
14. Hedberg, L.; Hedberg, K.; Boltalina, O.V. ; Galeva, N.A.; Zapolskii, A.S.; Bagryantsev, V.F. *J.Phys.Chem.* 108 A, 4731 (2004).
15. Chang, A.H.H.; Ermler, W.C.; Pitzer R.M. *J. Phys. Chem.* 95, 9288 (1991).
16. Weaver, J.H.: *Acc. Chem. Res.* 25, 143 (1992).
17. Lee, B.X.; Cao, P.L. ; Que, D.L. *Phys Rev* 61B, 1685 (2000).
18. Nagase, S. *Pure Appl. Chem.* 65, 675 (1993).
19. Slanina, Z., Lee, S.L.: *Fullerene Sci.Technol.* 2 459 (1994).
20. Lee, B.X.; Jiang, M.; Cao, P.L. *J.Phys. Condens. Matter* 11, 8517 (1999).
21. Sheka, E.F., Chernozatonslii, L.A. *J. Phys. Chem. C*, 111, 10771 (2007).
22. Zayets, V.A. "CLUSTER-Z1: Quantum-Chemical Software for Calculations in the s,p-Basis", Institute of Surface Chemistry, Nat. Ac.Sci. of Ukraine: Kiev, 1990.
23. Weaver, J.H.; Martins, J.L.; Komeda, ; Chen, Y.; Ohno, T.R.; Kroll, G.H.;
24. Wang, X.-B.; Ding, C.-F.; Wang, L.-S. *J.Chem.Phys.* 110, 8217 (1999).
25. Overhauser, A.W. *Phys.Rev.Letts.* 4, 415, 466 (1960).
26. Touless, D.J. *The Quantum Mechanics of Many-Body Systems*. AP: NY, 1961
27. Adams, W.H. *Phys.Rev.* 127, 1650 (1962).
28. Löwdin, P.O. *Phys. Rev.* 97, 1509 (1955).
29. Koutecki, J. *J.Chem.Phys.* 46, 2443 (1967).
30. Čížek, J.; Paldus, J. *J.Chem.Phys.* 47, 3976 (1967).
31. Benard, M. *J.Chem.Phys.* 71, 2546 (1979).
32. Paldus, J.; Veillard, A. *Mol. Phys.* 35, 445 (1978).
33. Ermer, O. *Angew. Chem. Int. Ed. Engl.* 26, 782 (1987).
34. Wiberg, K.B. *Tetrahedron* 24, 1083 (1968).
35. Orlandi, G.; Negri, F. *Photochem. Photobiol. Sci.* 1, 289 (2002).
36. Horoyski, P.J.; Thewalt, M.L.W.; Anthony, T.R. *Phys. Rev. B* 54, 920 (1996).
37. Shpol'skii, E.V. *Soviet Physics-Uspekhi* 77, 321 (1962).
38. Razbirin B.S.; Starukhin A.N.; Nelson D.K.; Sheka E.F.; Prato M. *Int. Journ. Quant. Chem.* 107, 2787 (2007).
39. Razbirin B.S.; Sheka E.F.; Starukhin A.N.; Nelson D.K.; Troshin P.A.; Lyubovskaya R.N. *Phys. Sol. State* 51, 1315 (2009).
40. Sheka E. F.; Razbirin B. S.; Starukhin A. N.; Nelson D. K., Degunov M. Yu.; Fazleeva G. M.; Gubskaya V. P.; Nuretdinov I. A. *Phys. Sol. State* 51, 2193 (2009).

41. Broude, V.L.; Rashba, E.I.; Sheka, E.F. *Spectroscopy of Molecular Excitons*. Springer: Berlin (1985).
42. Osadko, I.S. *Physics-Uspekhi*, 22, 311 (1979).
43. Zabrodski H.; Peleg, S.; Avnir, D. *J. Amer. Chem. Soc.* 114, 7843 (1992).
44. Zabrodski H.; Peleg, S.; Avnir, D. *J. Amer. Chem. Soc.* 115, 8278 (1993).
45. Pinsky, M.; Dryzun, C.; Casanova, D.; Alemany P.; Avnir, D. *J. Comp. Chem.* 29, 2712 (2008).
46. Zabrodsky, H.; Avnir, D. *J. Am. Chem. Soc.* 117, 462 (1995).
47. Pinsky, M.; Avnir, D. *Inorg. Chem.* 37, 5575 (1998).
48. Alvarez, S.; Avnir, D.; Llunell, M.; Pinsky, M. *New J. Chem.* 26, 996 (2002).
49. Alikhanidi, S.; Kuz'min, V. *Zh. Strukt. Khimii* 1998, 39, 548.
50. Alikhanidi, S.; Kuz'min, V. *J. Mol. Mod.* 1999, 5, 116/
51. Tratch, S. S.; Zefirov, N. S. *J. Chem. Inf. Comp. Sci.* 38, 331 (1998).
52. Grimm, S. *Chem. Phys. Lett.* 1998, 297, 15.
53. Petitjean, M. *Entropy* 5, 271 (2003).
54. Avnir, D.; Dryzhun, C. *Phys. Chem. Chem. Phys.* 11, 9653 (2009).
55. Estrada, E.; Avnir, D. *J. Amer. Chem. Soc.* 125, 4368 (2003).
56. Avnir, D.; Katzenelson, O.; Keinan, S.; Pinsky, M. Salomon, Y.; Zabrodsy. In *Concept in Chemistry. A Contemporary Challenge*; Rouray, D. Ed. John Wiley and Sons: New York, p.283 (1997).
57. Keinan, S.; Avnir, D. *J. Amer. Chem. Soc.* 120, 6152 (1998).
58. Katzenelson, O.; Avnir, D. *Chem.-Eur. J.* 6, 1346 (2000).
59. SHAPE, SYMMETRY, and CHIRALITY programs. (2010).
<http://www.csm.huji.ac.il/new/>
60. M. Zerner, *Reviews in Computational Chemistry*, Volume 2, Eds. K. B. Lipkowitz and D. B. Boyd, VCH, New York, 313, (1991).
61. Frisch, M. J.; Trucks, G. W.; Schlegel, H. B.; Scuseria, G. E.; Robb, M. A.; Cheeseman, J. R.; Montgomery, Jr., J. A.; Vreven, T.; Kudin, K. N.; Burant, J. C.; Millam, J. M.; Iyengar, S. S.; Tomasi, J.; Barone, V.; Mennucci, B.; Cossi, M.; Scalmani, G.; Rega, N.; Petersson, G. A.; Nakatsuji, H.; Hada, M.; Ehara, M.; Toyota, K.; Fukuda, R.; Hasegawa, J.; Ishida, M.; Nakajima, T.; Honda, Y.; Kitao, O.; Nakai, H.; Klene, M.; Li, X.; Knox, J. E.; Hratchian, H. P.; Cross, J. B.; Bakken, V.; Adamo, C.; Jaramillo, J.; Gomperts, R.; Stratmann, R. E.; Yazyev, O.; Austin, A. J.; Cammi, R.; Pomelli, C.; Ochterski, J. W.; Ayala, P. Y.; Morokuma, K.; Voth, G. A.; Salvador, P.; Dannenberg, J. J.; Zakrzewski, V. G.; Dapprich, S.; Daniels, A. D.; Strain, M. C.; Farkas, O.; Malick, D. K.; Rabuck, A. D.; Raghavachari, K.; Foresman, J. B.; Ortiz, J. V.; Cui, Q.; Baboul, A. G.; Clifford, S.; Cioslowski, J.; Stefanov, B. B.; Liu, G.; Liashenko, A.; Piskorz, P.; Komaromi, I.; Martin, R. L.; Fox, D. J.; Keith, T.; Al-Laham, M. A.; Peng, C. Y.; Nanayakkara, A.; Challacombe, M.; Gill, P. M. W.; Johnson, B.; Chen, W.; Wong, M. W.; Gonzalez, C.; and Pople, J. A. *Gaussian 03 (Revision B.03)*; Gaussian Inc., Pittsburgh PA (2003).
62. Sheka, E.F.; Razbirin, B.S.; Starukhin, A.N.; Nelson, D.K.; Degunov, M.Yu.; Troshin, P.A.; Lyubovskaya, R.N. *J. Nanophot. SPIE* 3, 033501 (2009)

Table 1 Experimental data on C-C bond lengths of the C₆₀ molecule, Å

Experiment ¹⁾	Single C-C bonds (<i>p</i>)	Double C-C bonds (<i>h</i>)	Reference
EGD (<i>I_h</i>)	1.455(6)	1.398(10)	[9]
ND (powder) (<i>I_h</i>)	1.452(66)	1.391(63)	[10]
XRD (<i>I_h</i>)	1.452(66)	1.391(63)	[11]
¹³ C NMR (<i>I_h</i>)	1.450 (15)	1.400 (15)	[12]
QCh (UBS HF AM1) (<i>C_i</i>)	1.464(13)	1.391(32)	[13]
QCh (RHF AM1) (<i>I_h</i>)	1.463(3)	1.385(0.4)	[13]

Note 1: Uncertainties of physical experiments and dispersions of the C-C bond distributions provided by UBS HF AM1 calculations are given in parentheses.

Table 2 Characteristics of singlet ground state of fullerenes [13] ¹⁾.

Solution / Data		C ₆₀	C ₇₀	Si ₆₀
RHF	Heat of formation ²⁾ , <i>kcal/mol</i>	970.180	1061.136	1295.967
	Symmetry	<i>I_h</i>	<i>D_{5h}</i>	<i>C_i</i>
	Number of effectively unpaired electrons, <i>e</i>	0	0	0
	Total spin $\langle \hat{S}^2 \rangle$	0	0	0
	Ionization potential ³⁾ , <i>I</i> , eV	9.64	9.14	8.00
	Electron affinity ³⁾ , ϵ , eV	2.95	3.27	3.38
UBS HF	Heat of formation ²⁾ , <i>kcal/mol</i>	955.362	1020.226	1011.722
	Symmetry	<i>C_i</i>	<i>D_{5h}</i>	<i>C_i</i>
	Number of effectively unpaired electrons, <i>e</i>	9.84	14.40	63.52
	Total spin $\langle \hat{S}^2 \rangle$	4.92	7.20	31.76
	ΔE^{RU} , <i>kcal/mol</i>	14.818	40.910	284.245
	Ionization potential ³⁾ , <i>I</i> , eV	9.87 (8.74 ^a)	9.87	8.98
	Electron affinity ³⁾ , ϵ , eV	2.66 (2.69 ^b)	2.73	2.70
Pure spin state	Heat of formation, <i>kcal/mol</i>	899.580	963.176	994.597
	Symmetry	<i>C_i</i>	<i>D_{5h}</i>	<i>C_i</i>
	Number of effectively unpaired electrons, <i>e</i>	0	0	0
	Total spin $\langle \hat{S}^2 \rangle$	0	0	0
	ΔE^{RPS} ⁴⁾ , <i>kcal/mol</i>	70.600	97.960	314.903

¹⁾ Data were obtained by using RHF and UHF versions of the AM1 semi-empirical technique implemented in the CLUSTER-Z1 software [22]. UHF presents a single-determinant broken symmetry unrestricted Hartree-Fock approach.

²⁾ Molecular energies are presented by heats of formation ΔH determined as $\Delta H = E_{tot} - \sum_A (E_{elec}^A + EHEAT^A)$. Here $E_{tot} = E_{elec} + E_{nuc}$, while E_{elec} and E_{nuc} are the electron and core energies. E_{elec}^A and $EHEAT^A$ are electron energy and heat of formation of an isolated atom, respectively.

³⁾ Here ionization potential and electron affinity correspond to energies of HOMO and LUMO, respectively, just inverted by sign. Experimental data for relevant orbitals of C₆₀ are taken from [23] (a) and [24] (b).

⁴⁾ ΔE^{RPS} presents the difference between the heats of formation of RHF and pure spin states.

Table 3 Continuous symmetry measures S_y related to element symmetry of I_h point group ¹⁾

Molecule	E	C5	C3	C2	i	S10	S6	σ (Ch)
C60_RHF	0	0	0	0	0	0	0	0
C60_UBS HF	0	0.000093	0.000085	0.000054	0.000056	0.00011	0.0001	0.000056
I	0	0.097742	0.058939	0.374478	0.945437	0.47872	0.42051	0.033549
I_sk	0	0.000231	0.000186	0.000128	0.000132	0.00024	0.00023	0.000132
II	0	0.040622	0.034247	0.0007	0.064343	0.14461	0.06438	0.025276
II_sk	0	0.000094	0.000086	0.000057	0.000058	0.0001	0.00011	0.000056
III	0	0.041919	0.050337	0.036587	0.363893	0.39697	0.39599	0.0193
III_sk	0	0.000102	0.000092	0.000067	0.00006	0.00011	0.00011	0.00006
IV	0	0.056269	0.032465	0.032465	0.987355	0.35785	0.35683	0
IV_sk	0	0.000215	0.000159	0.000121	0.000121	0.00023	0.00022	0.000121
V	0	0.101112	0.068744	0.042874	0.877885	0.63536	0.5452	0.159748
V_sk	0	0.000225	0.000165	0.000126	0.000127	0.00024	0.00023	0.000127

¹⁾Equilibrium structures of species molecules are given in Fig.3. Addition 'sk' marks 60-atom fullerene skeleton of the corresponding derivatives.

Table 4 Classical and continuous symmetry numbers of fullerene C₆₀ and its monoderivatives ¹⁾

Molecule	Symmetry	σ classic	σ continuous		Total
			E + Cn	i + Sn + σ	
C60_RHF	<i>Ih</i>	120	60	60	120
C60_UBS HF	<i>Ci</i>	2	59.995	59.994	119.99
I	<i>CI</i>	1	50.858	38.652	89.51
I_sk	<i>CI</i>	1	59.989	59.987	119.976
II	<i>CI</i>	1	58.33	54.798	113.1279
II_sk	<i>CI</i>	1	59.995	59.994	119.989
III	<i>CI</i>	1	57.438	41.899	99.338
III_sk	<i>CI</i>	1	59.995	59.994	119.989
IV	<i>CI</i>	1	57.513	43.288	100.801
IV_sk	<i>CI</i>	1	59.99	59.988	119.978
V	<i>CI</i>	1	55.555	30.573	86.129
V_sk	<i>CI</i>	1	59.989	59.988	119.977

¹⁾ See footnote to Table 3.

Table 5. Percentage contribution of the addend atoms into HOMOs and LUMOs¹⁾

Molecule	HOMO	LUMO
I	1.4	0
II	0	0
III	0.9	0
IV	1.0	0
V	97.1	0

¹⁾ See footnote 1 to Table 3

Table 6. Calculated energies of the lowest excited states and oscillator strengths of the lowest electronic transitions (ZINDO/S)

Molecule	Energy, eV	Oscillator strength
C ₆₀ -RHF	2.2394	0
	2.2414	0
	2.2429	0
	2.3156	0
	2.3163	0
	Σ	0
C ₆₀ -UBS HF	2.0785	0
	2.1456	0
	2.1458	0
	2.2217	0
	2.2856	0
	Σ	0
I	1.9712	0.0098
	1.9898	0.0004
	2.1897	0.0001
	2.1897	0.0001
	2.2506	0.0003
	Σ	0.0107
II	2.0120	0
	2.0490	0.0043
	2.1440	0
	2.225	0.0003
	2.3	0.0001
	Σ	0.0047
III	2.0548	0.0002
	2.1073	0
	2.1417	0.0061
	2.2226	0
	2.3314	0.0001
	Σ	0.0064
IV	2.0487	0.0004
	2.0782	0.0001
	2.0840	0.0096
	2.1926	0
	2.3559	0.0002
	Σ	0.0103
V	2.0445	0.0007
	2.0636	0.0022
	2.0778	0.0090
	2.1839	0.0003
	2.3538	0.0003
	Σ	0.0125

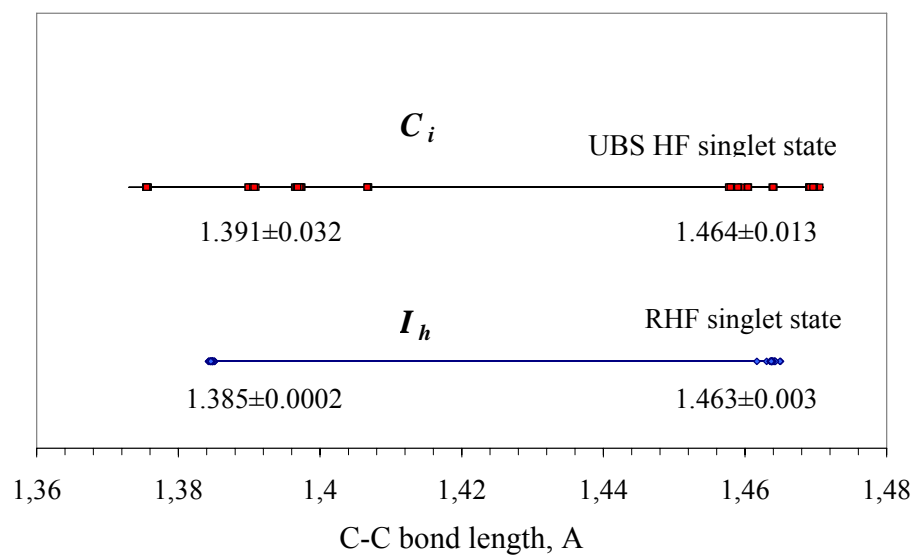


Figure 1. Dispersion of the C-C bonds of the C_{60} molecule [15].

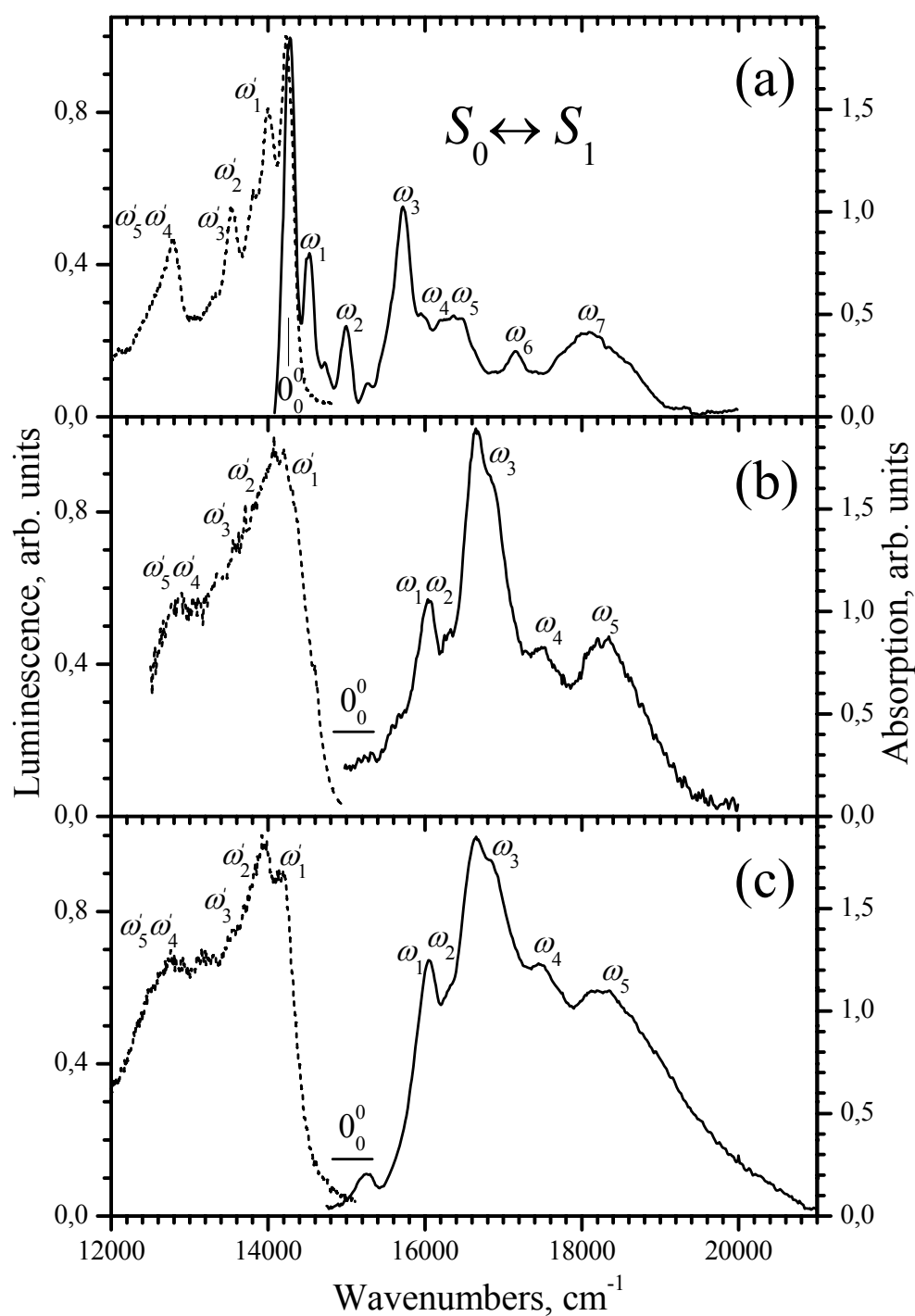


Figure 2. Specular background-free absorption (solid lines) and luminescence (dotted lines) spectra of **I** (a), **II** (b), and C_{60} (c) in crystalline toluene ($T = 80$ K). ω_i and ω'_i Mark vibronic bands in the absorption and luminescence spectra, respectively. Vibrational analysis of the vibronic series is presented in [38]. 0_0^0 Marks the position of a pure electronic transition which is quite certain for **I** and fills some regions for **II** and C_{60} due to multiplet structure.

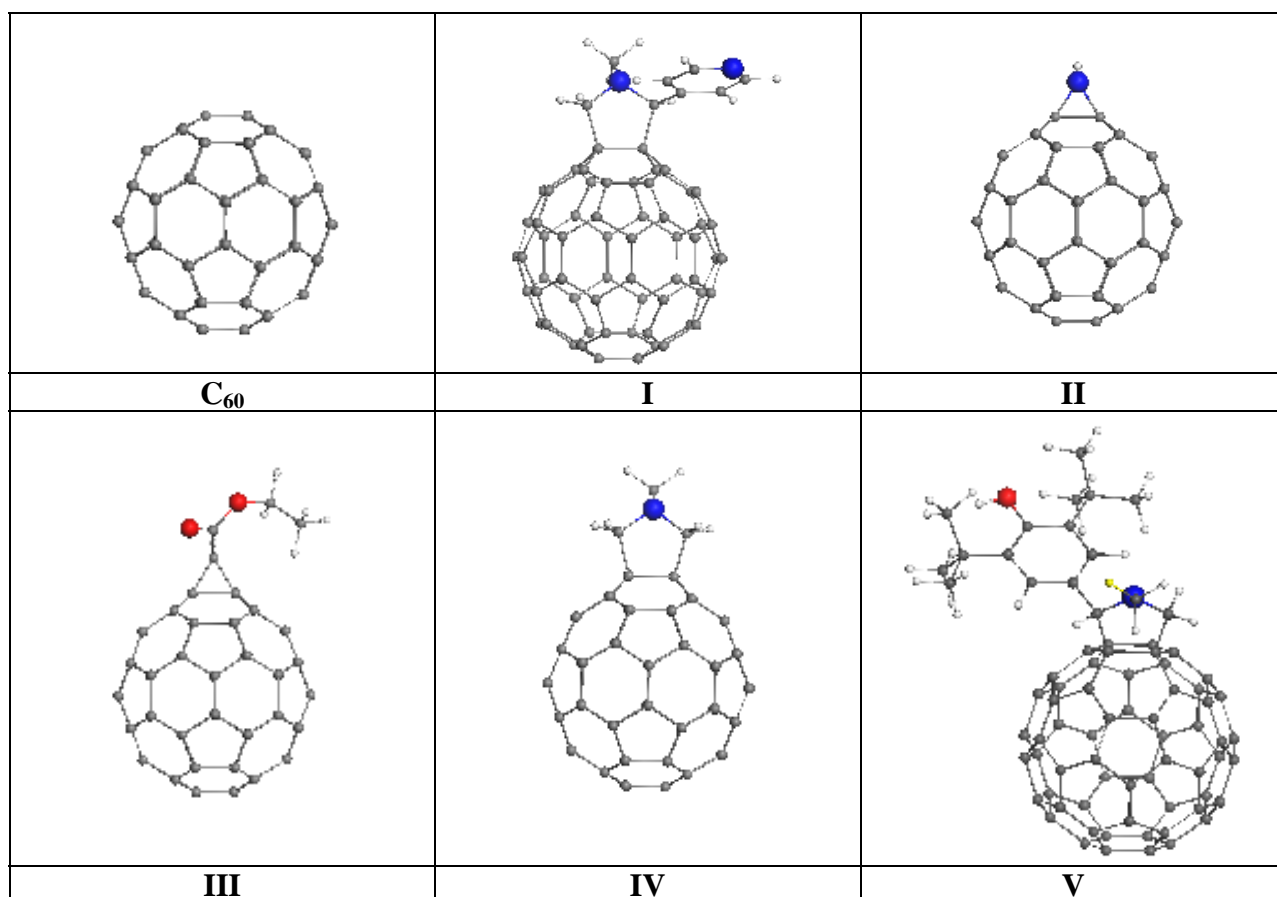


Figure 3. Equilibrium structures of fullerene C₆₀, N-methyl-2(4-pyridine)-3,4-[C₆₀]fulleropyrrolidine (**I**) [38], fullerene azyridine [C₆₀] (**II**), ethyl ester of [C₆₀]fullerene acetic acid (**III**) [39], N-methyl-3,4-[C₆₀]fulleropyrrolidine (**IV**) [39], and N-methyl-2-(3,5-di-*tert*-butyl-4-hydroxyphenyl)-[C₆₀] fulleropyrrolidine (**V**) [40]. Carbon atoms are not shown. Big blue and red balls mark nitrogen and oxygen atoms. Hydrogens are shown by small white balls. UBS HF, singlet state.

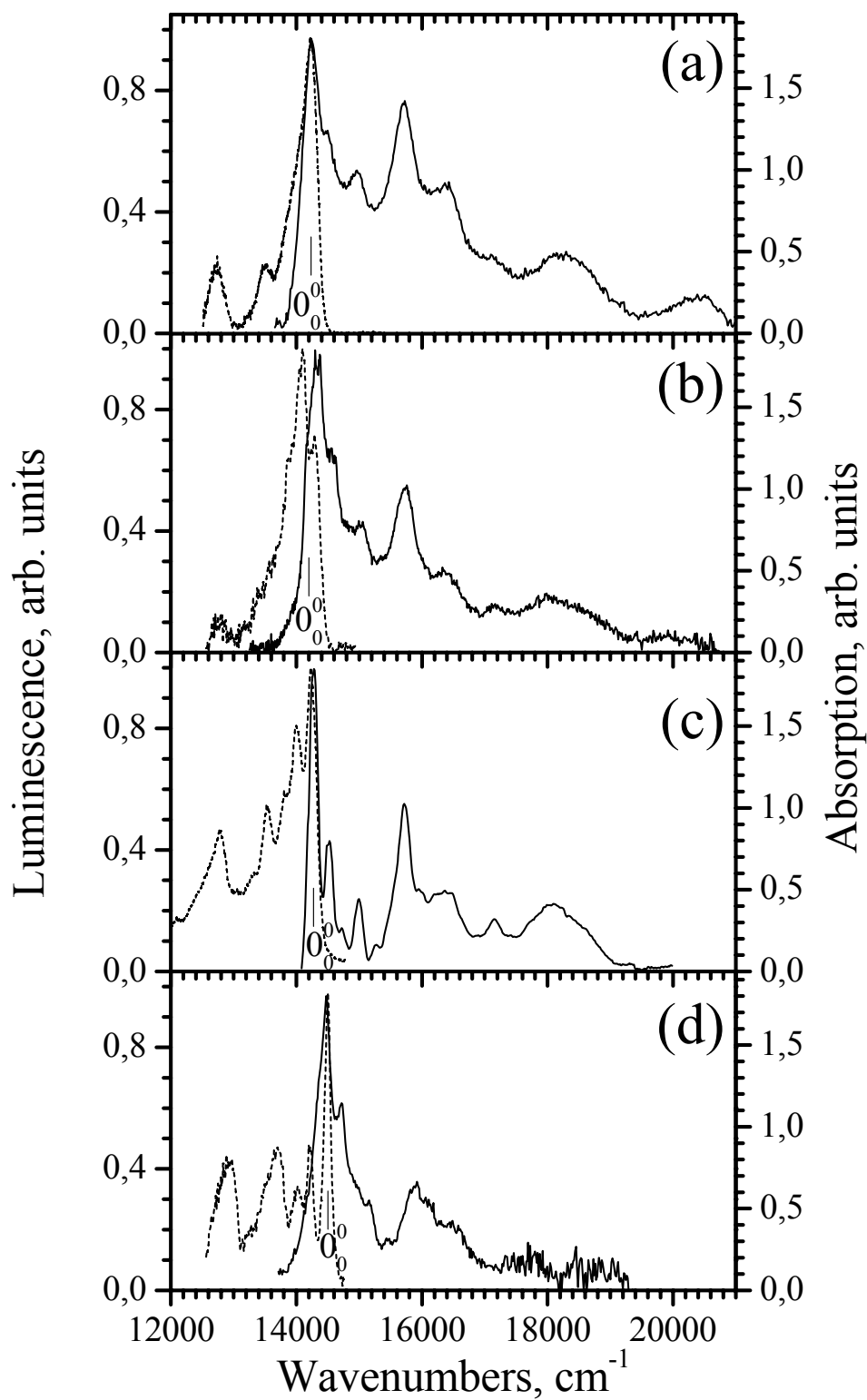


Figure 4. Specular background-free absorption (solid lines) and luminescence (dotted lines) spectra of **V** [40] (a), **I** (b) [38], **IV** [38] (c) and **III** [39] (d) in crystalline toluene ($T = 80$ K). 0_0^0 marks the positions of a pure electronic transitions.

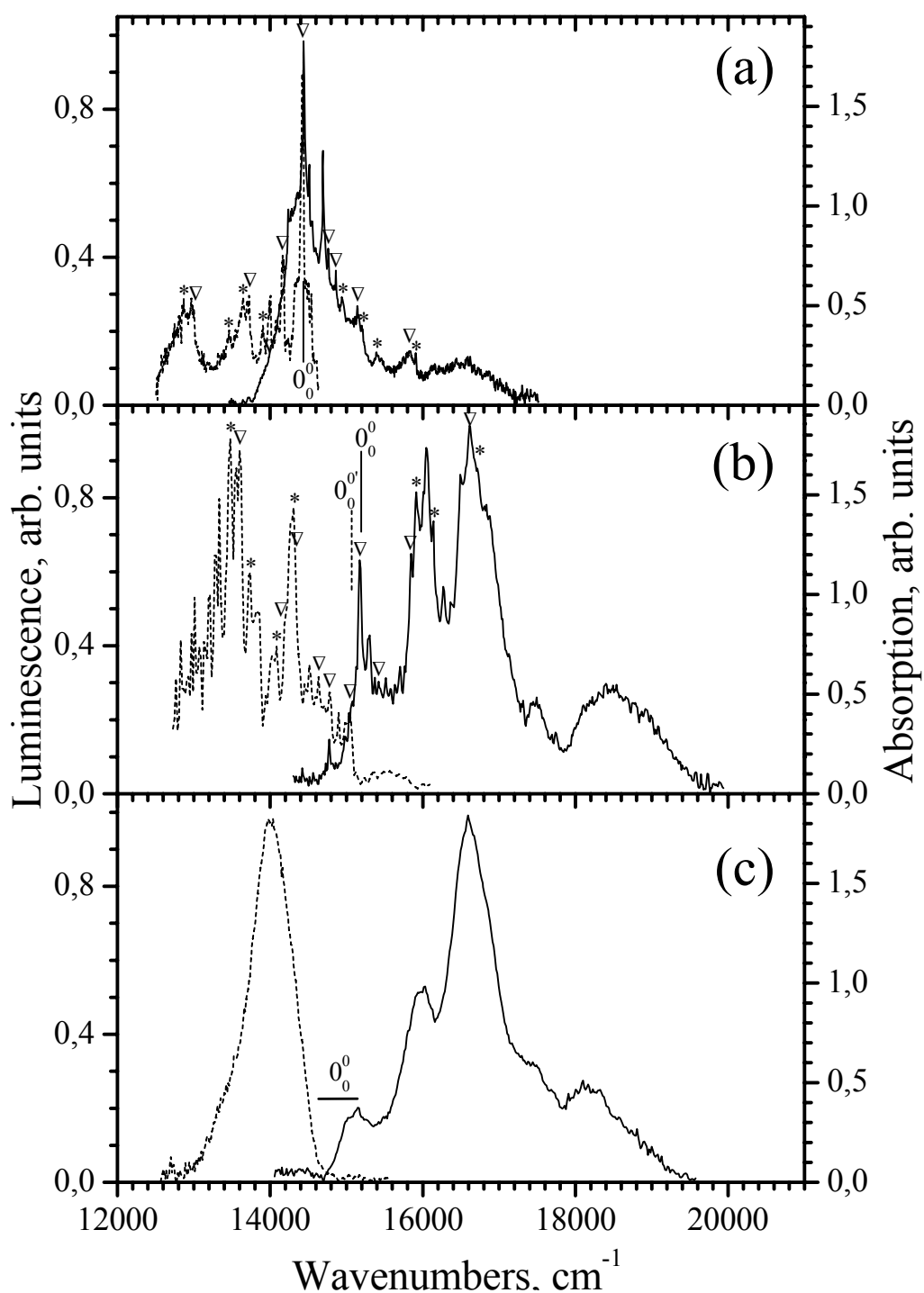


Figure 5. Specular background-free absorption (solid lines) and luminescence (dotted lines) spectra of **III** [39] (a), C_{60} [38] (b), and **II** (c) in crystalline toluene ($T = 2$ K). 0_0^0 and $0_0^{0'}$ mark the positions of pure electronic transitions. Stars and triangles mark vibronic bands related to the HT and FC series, respectively. The series separation is based on the vibrational analysis of the spectra given in Refs. 38-40.